2D Transition Metal Dichalcogenides for Energy-Efficient Two-Terminal Optoelectronic Synaptic Devices

Roshni Satheesh Babu¹, Dimitra Georgiadou^{1,2*1}

¹School of Electronics and Computer Science, University of Southampton, Southampton SO17 1BJ, United Kingdom

² Optoelectronics Research Centre, University of Southampton, Southampton SO17 1BJ, United Kingdom

*d.georgiadou@soton.ac.uk

Summary

Two-dimensional layered transition metal dichalcogenides (2D TMDC), such as tungsten disulphide, molybdenum disulphide, compounds based on rhenium, and their heterostructures, have been used to fabricate artificial synaptic devices that combine memory, computation, and sensing in a single system. By using a combination of opto-/electronic signal processing systems, these devices have demonstrated multi-state memory, pattern recognition capabilities, biological synaptic behaviour, and visual information processing. Their advanced scalability and integration potential renders them ideal candidates for emerging neuromorphic memories in edge AI and wearable devices. Although ultra-low power consumption in neuromorphic vision systems in the range of femtojoule has been achieved, optimising the materials' quality and controlling the defect formation are still required to enhance their functionality and improve the devices' performance. Improving the scalability of heterostructures and integrating many single devices in arrays operating as part of a neuromorphic system is paramount to their commercialisation.

¹ Lead Contact: Dimitra G. Georgiadou, d.georgiadou@soton.ac.uk

Introduction

Two-dimensional (2D) transition metal dichalcogenides (TMDC) and their heterostructures have attracted attention in the emerging area of neuromorphic computing, due to their intriguing optoelectronic properties stemming from their low dimensionality.^{1,2} Light perception and cognition is an important sensory function for bioinspired electronics, for example, in artificial vision systems.³ The ability of 2D TMDC materials to combine electrical with optical operations enables development of synthetic retinas as well as optoelectronic interfaces for integrated photonic circuits.⁴

Optoelectronic artificial synapses co-locate the optical signal detection and memory functions in a single unit, being thus capable of sensing and memorising information, giving rise to humanoid optoelectronic devices. Compared to purely electrical artificial synapses, optoelectronic ones involve a noncontact writing method and could enhance the processing speed because of their high bandwidth and ultrafast signal transmission, critical for low power computation in edge AI applications. Moreover, low cross-talk can be obtained, owing to the photo-writing being orthogonal to the electrical readout, providing a spatially confined stimulation that can offer secure authentication in decentralised devices, like biometric systems.^{4,5}

In this Perspective, we discuss the optoelectronic synaptic devices, which are enabled by the strong light—matter coupling in 2D TMDC. These materials possess a highly tuneable band gap, which covers from visible to infrared, and undergo a direct-to-indirect band gap transition when increasing the number of layers from monolayer to bulk.⁶ The various energy band configurations that can be designed by engineering van der Waals (vdW) homo-or heterostructures⁷ open new avenues to the development of opto-/electronic synaptic and heterosynaptic devices. As an example, monolayers with <1nm thickness of MoS₂, MoSe₂, and WS₂ can absorb up to 5–10% incident sunlight, which represents more than 10-fold increase in sunlight absorption than GaAs and Si, the common materials used in solar cells.⁸

Next, we summarise some key optical properties of the main TMDC materials that are being used in optoelectronic synaptic applications. Then, we explore how these materials have been incorporated in optoelectronic neuromorphic applications. We focus on two-terminal devices, which we believe are advantageous to transistors in terms of higher integration into dense crossbar arrays, simpler fabrication and faster switching speed. The extra degree of freedom for

programming and controlling neuromorphic operation that is provided by the gate terminal in mem-transistors is replaced by an optical source (acting as the gate) in the optoelectronic two-terminal devices. We introduce the operating mechanism and transport phenomena in TMDC-based optoelectronic memristive devices and then we showcase representative examples of emerging applications realised with single layer TMDC and TMDC heterostructures, comprising either different TMDC or a TMDC material and an oxide layer.

Transition Metal Dichalcogenide Materials Considerations

TMDC are layered materials with stoichiometry MX₂, where M is a transition metal atom and X is a chalcogen. The transition metals encountered in TMDC usually belong to groups IVB (titanium, Ti; zirconium, Zr; hafnium, Hf), VB (vanadium, V; niobium, Nb; tantalum, Ta), VIB (molybdenum, Mo; tungsten, W), VIIB (technetium, Tc; rhenium, Re) and VIIIB (palladium, Pd; platinum, Pt), while the most commonly employed chalcogen elements from group VIA are sulphur (S), selenium (Se) and tellurium (Te) (see Figure 1A). TMDC thin films are composed of a layer of metal atoms sandwiched between two atomic layers of the chalcogen. The atoms in the MX₂ structure are covalently bonded and the layers are stacked together by weak van der Waals bonds. The transition metal atom contributes four electrons to bond with chalcogen atoms, resulting in oxidation states of +4 for the transition metal and -2 for the chalcogen atom. 9 MX₂ monolayers can exist in three phases, namely 1T, 2H and 3R, where numbers represent the number of layers in the unit cell and the letters T, H, and R indicate trigonal prismatic, hexagonal, and rhombohedral symmetry, respectively, examples shown in Figure 1B. The structural phase transitions that can be achieved between these polymorphs can give rise to a multitude of reliable and fast switching states, similar to those induced by ion migration in resistive random access memories (RRAMs) and by amorphous-to-crystalline transitions encountered in phase change materials (PCMs).¹⁰

Tungsten disulphide (WS₂) is a well-known TMDC material with intriguing optoelectronic properties that involve high optical absorption coefficient (in a broad spectrum region from visible to the near-infrared), high carrier mobility, high aspect ratio, and excellent thermal and chemical stability.¹¹ The band gap of bulk and monolayer WS₂ are 1.3 eV (indirect) and 2.1 eV (direct), respectively.¹² The energy band of WS₂ shows a noticeable split in the valence band at the K point

caused by the spin-orbit coupling.¹³ This leads to a strong photoluminescence and a large light absorption coefficient.

Another critical material used in optoelectronic applications is molybdenum disulphide (MoS₂), which has a unique crystal structure consisting of covalently bonded molybdenum and sulphur atoms, with layers spaced apart by approximately 6.5 Å and held together by van der Waals forces.¹⁴ MoS₂ exhibits a tuneable band gap, approximately 1.2 eV for bulk and 1.8 eV for monolayer, as well as high carrier mobility.¹⁵ Molybdenum diselenide (MoSe₂) has 1.1 eV indirect band gap in bulk films and 1.5 eV direct band gap in its monolayer structure, slightly smaller than MoS₂ due to the effect of the chalcogen (Se) atom p_z orbital in the valence band maxima.¹⁶ Similar to WS₂, MoS₂ and MoSe₂, the bandgap of MoTe₂ can also be tuned, although at smaller scale (1.0 eV and 1.1 eV for bulk and single layer, respectively).¹⁷

Rhenium based materials, such as rhenium disulphide (ReS₂) and rhenium diselenide (ReSe₂), exhibit slightly different properties, owing to their weaker interlayer coupling. ReS₂ maintains the characteristics of a direct band gap semiconductor across different layer numbers, showing stable optical properties and a bandgap of around 1.5-1.6 eV.¹⁸ Similarly, ReSe₂, which is of isoelectronic nature with ReS₂, shows potential for further tuning of magnetic and optical properties via strain engineering due to its lattice distortion, while its bandgap is weakly layer-dependent and decreases from 1.31 eV for thin layers to 1.29 eV in thick flakes.¹⁹ The stability of the optical properties with increasing number of layers gives these materials a technological advantage over other 2D materials, as a monolayer is not required for a direct bandgap.²⁰

TMDC Optoelectronic Neuromorphic Applications

Operating mechanisms of TMDC-based optoelectronic devices

Optoelectronic synaptic devices that integrate both optical and electrical stimulation to process and store information have opened new outlook in neuromorphic computing. The key components of an optoelectronic synaptic device involve input stimulation, signal detection and processing, synaptic weighting and signal output. The input stimulation can be electrical (current or voltage) and/or optical signals. The use of optical signal as the input stimulus offers major benefits, such as low power consumption, minimal signal interference (low crosstalk), high bandwidth, and avoids

delay caused by resistance-capacitance (RC), which are common pitfalls encountered in purely electrical inputs.⁵

There are various mechanisms responsible for the operation of a synaptic device, such as creation of conductive filaments, phase change, vacancy migration, and charge trapping/de-trapping.² Especially for an optoelectronic device that couples the optical and electrical stimulation to achieve the synaptic functionalities, photo-induced doping²¹ and trapping/de-trapping²² of photogenerated charge carriers at the interfaces or defect sites are the main mechanisms responsible for the switching and for mimicking synaptic behaviours. By inducing trap sites in a TMDC, we can modify its conductivity, which is analogous to the modification of the synaptic weight.

Shallow trap levels are created by substitutional defects and are located around 10 meV of the valence or conduction band.²³ They enhance charge carrier mobility and result in fast switching speeds. On the contrary, deep traps, created from vacancies, span a range of 0.1-0.4 eV inside the band gap and are responsible for hysteresis, charge storage and long-term memory effects, as the optical information can be "remembered" by the retention of these trapped carriers even after the stimulus has been removed.²⁴ Grain boundaries, are impeding charge transport and serve as a spatial barrier where the vacancies accumulate, influencing the size and location of conducting filament formation in 2D memristive devices. By engineering the several types of defects in TMDC during synthesis or upon applying some type of post-treatment, one can control many of the properties that define the synaptic plasticity of the devices and their short- and long-term memory.

Interface-induced trap states occur near the semiconductor-dielectric boundary due to imperfections like structural irregularities or impurities, impacting the optoelectronic behaviour of devices by trapping carriers at the interface, and are often regulated through electric double layers (EDLs). Heterojunction-induced trap states arise in heterostructures, including van der Waals interfaces between different 2D materials, which are designed to improve charge separation, control charge trapping in specific layers, and optimise carrier transport via engineered band alignment.

Together, these mechanisms allow optoelectronic synaptic devices to couple optical and electrical signals, achieving complex synaptic functionalities and paving the way for advancements in neuromorphic computing and artificial intelligence hardware.

Single layer optoelectronic synaptic devices

A memristive device is a two terminal non-volatile memory device capable of remembering its resistance state induced by voltage or current applied to it, even after the original stimulus has been removed. The concept of the memristor was proposed by Chua in 1971,²⁵ and the first memristive device was demonstrated in 2008.²⁶ Such a device typically consists of three layers, two metal electrodes and a storage layer. The storage layer can be reconfigured by stimulating with either electrical or optical signals and can lead to memory effects. Recently, by controlling the volatility characteristics of a memristive device, it was found that both neuronal and synaptic behaviours can be emulated.²⁷ Therefore, memristive devices are leading candidates for future neuromorphic computing systems by offering on-chip reconfigurable memory with high-density integration.²⁸ The *optoelectronic* memristive device integrates optical and electronic stimulus to achieve advanced data processing and memory capabilities that can closely mimic biological neural networks. Retinomorphic devices can perform image recognition tasks and be used in vision systems with ultra-low power consumption, while other neuronal functionalities, such as visual nociception can be also emulated. We have selected some representative examples from recent literature to position 2D TMDC materials at the forefront of this technology.

Retinomorphic devices and arrays

The retinomorphic devices mimic the way retina process the visual information. The retina captures the light signals via photoreceptor cells, called rods and cones, and the visual data is preprocessed through neural layers before transmitting it to brain *via* the optic nerve, ²⁹ as shown in **Figure 2A**. Recent advancements have demonstrated the potential of WS₂ to be employed in retinomorphic devices compatible with machine learning algorithms towards hardware-based artificial neural networks (ANNs). For instance, a 2D WS₂ retinomorphic memristive array was developed as part of an in-sensor reservoir computing system to facilitate the recognition and classification of traffic signals. ²⁹ The WS₂ memristive device (**Figure 2B**) demonstrated excellent optoelectronic synaptic properties, including excitatory postsynaptic current (EPSC), paired-pulse facilitation (PPF), short- and long-term potentiation (STP/LTP) characteristics, which are shown in **Figures 2C-F**. With this system, the handwritten numbers could be recognised with an accuracy of 88.3%, and 100% recognition rate for traffic signals of RGB wavelengths was achieved.

Image recognition

Taking advantage of the WS₂ capability for broadband light sensing, optoelectronic resistive memory devices performing image recognition tasks were fabricated.³⁰ The broad wavelength range from 360 to 950 nm serves as the optical stimulus, with the device being highly responsive to 950 nm at room temperature. Both electrical and optical stimuli were applied to control the SET/RESET behaviour of the WS₂ memristor. Potentiation and depression were achieved by applying 32 optical (2 sec, 90 μW cm⁻²) and electrical pulses (2 sec, -10 V), respectively. The WS₂ photonic synapses were used to recognise images from the Modified National Institute of Standards and Technology (MNIST) datasets and obtained an accuracy of 98.27%, showcasing the high potential of this material for integrated sensing and computing memory functionalities.

More "exotic" devices, such as the so-called "memitter" (memory-emitter), have been enabled by a monolayer WS₂, showing synaptic plasticity and visual memory characteristics.³¹ A memitter device is an all-optical neuromorphic type of data processing system, which utilises the adaptive photoluminescent (PL) (instead of adaptive resistance that typically occurs in memristors, i.e., memory resistors) response of WS₂ monolayer when exposed to optical stimulation. When WS₂ was exposed to continuous wave 520 nm laser irradiation, the PL intensity increased over time due to the reduction in the n-doping of WS2 resulting from electron transfer to the laser-induced adsorption of atmospheric molecules like O₂ and H₂O, and decreased gradually after removing the laser light stimulus or after applying engineered pulsed optical waves. The device demonstrated the memorisation and forgetting process that mimics biological synaptic behaviour upon monitoring the change in photoluminescence emission intensity. The WS₂ memitter performed short-term synaptic behaviour and spatial processing capabilities that render it suitable for storing the visual information. It supports pattern recognition and fading memory effects, akin to visual short-term memory (VSTM) of human brain and can serve as a platform for physical reservoir computing. The capability of the 2D memitter to sense, process, and memorise/forget optical inputs in the same physical substrate can be utilised for in-sensor computing. The incorporation of an insensor system could overcome the hardware bottleneck of using separate sensors and processors.

Optoelectronic operation of memristive devices can be further combined with other 2D TMDC material properties, such as ferroelectricity, for increased performance in image recognition tasks. In a report by Yan *et al.*, the fabricated ReSe₂ ferroelectric memristor with structure Pd/Al₂O₃/ReSe₂/SiO₂/Si was stimulated by both all-optical and electrical signals.³² When the

device is electrically or optically triggered, it switches between the high (HRS) and low resistive state (LRS), owing to the change in the barrier height at the Al₂O₃ and SiO₂ interfaces with the ReSe₂, caused by polarisation flipping in the ferroelectric 2D material. The device shows long-term potentiation and depression under the illumination with visible light, although the linearity of the weight update (i.e., conductance change) were 0.94 and 0.88 for potentiation and depression, respectively, which was lower than the ones achieved for electrical-only input pulses (0.99 and 0.98). This high linearity resulted in an error rate of 2.96% when the ReSe₂ ferroelectric synapses data were inserted in a training and inference simulation algorithm, implementing a six-layer convolutional neural network (CNN) using handwritten digit datasets from the MNIST database for image recognition. For reference, the error rate of digital recognition based on the ideal synaptic CNN was 1.15%.

Neuromorphic vision system (NVS) with ultra-low power consumption

One of the grand challenges that novel materials and device structures promise to address is the lowering of the power consumption of incumbent (Si-based) neuromorphic chips to the level of biological equivalent systems. To this end, Chen *et al.* fabricated a ReS₂ based optoelectronic synaptic memristor for a neuromorphic vision system (NVS) with ultra-low power consumption of about 12.2 fJ.³³ Unlike traditional vision systems, which mainly handle 2D images, their device enables 3D object recognition (stereo vision) by the fusion of its planar and depth images. The latter is formed by a conductance matrix that is based on distance detection due to different scattering of light from an object placed at various distances, which results in conductance changes. The ReS₂-based NVS device shows high recognition rate of 97.05% for 3D objects, when simulated using data from the optoelectronic ReS₂ synapses, and low accuracy recognition rate of 32.6% for 2D objects without the synapses inserted in the same network structure. These devices with stereo vision-like capabilities are suitable for applications requiring secure verification and prevention of 2D spoofing, such as face recognition and entrance guard systems.

Visual nociceptor

Along the lines of developing artificial neuronal systems akin to the biological eye and the image processing capabilities in the brain, nociception is another interesting concept that researchers attempted to emulate by designing intelligent electronic devices. Visual nociceptors are essential sensory neurons that send the pain signals to the visual cortex of the brain for processing. This

mechanism is responsible for protecting humans from potential harm, when dangerous environmental stimuli, such as intense light, exceed a certain threshold. Replicating these painsensing behaviours is crucial for emulating the advanced bionic vision systems in a simple design that integrates both sensing and processing into a single device. Wavelength-sensitive pain detection is also important for minimising potential harm and improving the design of bionic vision systems. The intensity threshold for light causing retinal damage decreases for shorter wavelengths. If the eye has been already exposed/damaged by shorter wavelength, even the harmless longer wavelength light can lead to secondary damage.

A monolayer MoS₂ was employed to fabricate a wavelength-sensitive artificial "nociceptor" that integrates both sensing and processing capabilities.³⁴ The optical synaptic device demonstrates persistent photoconductivity (PPC) upon illumination, owing to the existence of dangling bonds and charged impurities at the MoS₂/SiO₂ interface, which allows emulation of synaptic functions, such as PPF, STP to LTP transitions and memorising/forgetting behaviours. The device also exhibits the wavelength-sensitive visual nociceptor functions, such as threshold detection, no adaptation to harmful stimulus and relaxation, as well as allodynia and hyperalgesia, which are shown in **Figure 3**. Due to the PPC effect, the longer the optical pulse and the greater its intensity, the higher the photocurrent produced, as more electron-hole pairs are generated, therefore the nociceptor threshold is crossed (akin to the feeling of pain in humans). This threshold is, however, wavelength-dependent, as the absorptance of the material is not constant across the whole visible spectrum but, same as the human eye, the damage is higher (i.e., the threshold is reached at lower intensities) when exposed to shorter wavelengths (for the same amount of time).

TMDC-based heterostructure devices

The simple fabrication of devices comprising a single semiconducting layer of a 2D TMDC material, using minimum process steps, has obvious advantages, that's why most reports so far are including these structures. However, heterostructures comprising at least one 2D TMDC, albeit more challenging to fabricate, as they require extra steps for the heterostructure assembly and alignment, provide access to new properties and applications beyond their single components' characteristics. These heterostructures offer multifunctionality and can respond to multiwavelength illumination, due to tailoring of their optical properties through band gap engineering.

More specifically, van der Waals (vdW) heterostructures consist of stacked 2D materials integrated with one-dimensional (1D), 2D, or three-dimensional (3D) bulk materials held together by weak vdW forces.³⁵ These structures feature atomically sharp interfaces, minimal lattice mismatch, and tuneable optical and electronic properties.³⁶ The absence of dangling bonds at the interfaces minimises defect-induced scattering and recombination and enhances the properties of optoelectronic devices.³⁷ The in-plane migration of intrinsic defects that occurs in heterosynaptic connections is very attractive for realistically emulating biological neural networks.

TMDC materials can form heterostructures with other TMDC or with semiconducting metal oxides. A MoS₂/cerium oxide (CeO₂) heterojunction was demonstrated that integrates a multifunctional artificial visual system with electrical storage, light sensing and memory, and visual nociceptors.³⁸ The authors demonstrated both electric- and light-induced synaptic plasticity. The change in conductance variation was studied and a 9×9 memristor array was used to sense and memorise images with the aid of a UV light stimulus with voltage-assisted modulation. In addition, a 7×7 optoelectronic memristor array was used to emulate the human vision for traffic signal, using multi-wavelength optical modulation (620 nm, 580 nm, and 520 nm), while they also demonstrated visual nociceptors. The features of biological nociceptor, such as threshold, no adaptation, relaxation, and sensitisation, were realised. CeO₂ exhibits strong absorption in the UV band but the presence of oxygen defects and excitation of electrons into the conduction band under the photoelectric effect contribute to its photo-response at visible wavelengths.

By taking advantage of the distinct optical properties of both materials, a MoS₂/zinc oxide (ZnO) heterostructure was employed in multi-wavelength sensing and memory.³⁹ This heterostructure device can sense UV, blue, green, and red light by using the oxygen dissociation of annealed ZnO (UV and visible light environment) and the persistent photoconductivity effect of MoS₂ in the visible light. The device senses and memorises UV light due to photogenerated carriers and changes in depletion region due to oxygen dissociation. For visible light, sensing and memory are enabled by trap states in MoS₂ and increased oxygen vacancies in ZnO nanowires upon annealing. The basic synaptic functions, such as EPSC, PPF, STP and LTP, were achieved, and the device could also emulate a wavelength-sensitive nociceptor.

Most TMDC materials are n-type semiconductors, same as the majority of metal oxides, therefore heterojunctions like the ones mentioned above cannot form p-n junctions that are suitable for

efficient photodetection, as is the case of in-memory light-sensing applications. To this end, Li *et al.* fabricated a Phosphorus (P)-doped MoSe₂/phosphorous oxide (P_xO_y) heterostructure by depositing partially oxidised black phosphorus (BP) on Mo and controllably selenising it.⁴⁰ The resulting bilayer of p-type P-MoSe₂ and n-type P_xO_y formed a p-n junction that was used for efficient separation of photogenerated electron-hole pairs. When light with wavelength 470-655 nm was shone on the heterojunction, the presence of the oxygen vacancies and photogenerated carriers contributed to the modulation of conductance, which is a key factor in the synaptic behaviour of the memristor.

vdW heterostructures comprising two distinct 2D TMDCs can deliver higher performance than their single counterparts. For example, a ReS₂/WS₂ based planar memristive device showed a higher switching ratio of 10⁶ than the single ReS₂ memristive devices, better endurance and retention, and higher integration density. The resistive switching in the memristive device occurs due to the formation of conducting filaments by sulphur (S) vacancies. The ReS₂ layer generates more S vacancies due to their lower stoichiometric ratio than WS₂. Therefore, the resistive switching is more dominant in the ReS₂ layer, while the WS₂ layer maintains the HRS. The heterostructure memristive device emulated the biological synapses, with S vacancies acting as the neurotransmitters in biological synapses, and voltage pulses acting as the stimulus signals. Because of the interlayer coupling and charge transfer of ReS₂/WS₂ heterostructure, it exhibits photoresponsive behaviour, therefore this structure can emulate optoelectronic memristor characteristics as well. The conductance level changed with the optical power density, showing the optical tunability of synaptic weight under 532 nm light stimulus. This kind of structures can be implemented in future visual neural applications.

The interfaces of 2D TMDC heterostructures can be engineered to comprise defects that enhance the optoelectronic properties of memristive synaptic devices. For instance, by exposing the MoS₂ layer to UV-ozone, Mo-O bonds are formed, and these lattice defects in the MoS_{2-x}O_x can be utilised to facilitate ion migration in MoTe₂/MoS_{2-x}O_x vdW heterostructures (**Figure 4A**). This heterostructure leverages the domain lifting effect of oxygen ion defect states in MoS_{2-x}O_x and narrow absorption band gap of MoTe₂ to enhance the carrier transport (**Figure 4B**). The short- and long-term depression and potentiation were achieved shining the visible (532 nm) and NIR (1064 nm) laser on top of the MoS_{2-x}O_x and MoTe₂, respectively. A high accuracy rate of 99.3%

was achieved for the electronic synapses and of 96.5% for the photonic synapses in recognising MNIST handwritten digits, while the accuracy was lower for recognition of flower images, namely 95.3% and 91.5%, respectively. The improved accuracy of the electrical synapses is attributed to the higher linearity of their conducting states.

Another interesting approach is to merge optical response with other functionalities that can enable multi-modal sensing in future intelligent electronic devices. Hou *et al.* fabricated a MoS₂/WSe₂ van der Waals heterojunction to replicate artificial visual synapses by utilising the photoconductivity (current response caused by light) and pyroconductivity (current response caused by temperature rise) mechanism.⁴³ The vdW heterojunction exhibits broadband synaptic behaviour from visible to infrared region (405-1064 nm) with low power consumption of 0.3-1.1 pJ per spike. The MoS₂/WSe₂ vdW heterojunction has lower power consumption than the single layer MoS₂ and WSe₂ devices, as the built-in field at the heterointerface results in lower dark current, which in turn improves the optical detection performance. Additionally, the pyroconductivity observed in the MoS₂/WSe₂ vdW heterojunction improved the synaptic performance, as it stabilises the post-synaptic current created after illumination for longer time after the light is turned off, as the temperature does not return to room temperature instantly.

Conclusions and Outlook

Inspired by the biological neural network, optoelectronic synaptic devices are opening new horizons in neuromorphic computing. 2D transition metal dichalcogenides and their heterostructures are potential candidates for optoelectronic synaptic devices because of their unique physical and chemical properties, such as layered structure and bandgap tunability, strong light-matter interaction, high carrier mobility and switching speed, broad spectral response, and energy efficiency. The atomically thin nature of these 2D materials provides an advantage for low operation voltage and ultra-low energy consumption (**Table 1**) as well as mechanical flexibility, attributes that are paramount in edge AI wearable devices, like smart lenses and artificial retinas to treat vision impairment or employed in robotics. For example, the Young's modulus (*E*) of monolayer MoS_2 is 25% that of graphene ($E_{MoS2} = 240$ GPa, $E_{graphene} = 1$ TPa), while their shear strength values are comparable (100-200 GPa). Despite the optical properties being slightly dependent on strain, this does not define their performance and it can be engineered to strengthen the optoelectronic performance of TMDC-based flexible devices and systems.

Their scalability potential to enable nanometre devices (as demonstrated by TSMC's monolayer MoS₂ nanosheet field-effect transistor with a gate length of 40 nm)⁴⁵ and their CMOS integration in large area substrates, as shown by imec's high-quality growth of WS₂ on 300 mm wafers using a modified metal-organic chemical vapor deposition (MOCVD) method⁴⁶ could further accelerate progress in the 2D neuromorphic memories.⁴⁷ However, as these are high temperature processes, transfer of the 2D layer after growth or alternative low-temperature and low-cost chemical exfoliation methods need to be considered for use with flexible (temperature-sensitive) substrates.⁴⁸

WS₂, MoS₂, WSe₂, and their various heterostructures have been used for the past couple of years and have advanced from research experiments to potential solutions for AI hardware and machine vision. The 2D TMDC-based optoelectronic synaptic devices can emulate brain-like synaptic behaviour and recognise patterns with extremely low power consumption (fJ). Optoelectronic or fully optical control has been achieved, while wavelength-sensitivity or broadband response can be obtained by choosing the suitable material from the wide range of existing layered transition metal dichalcogenides. Their rich optoelectronic properties allow the development of more exotic devices that can leverage their photoluminescence or ferroelectric characteristics.⁴⁹ Multimodal sensing is also possible as showcased in the photo- and pyroconductivity study. The large surface/volume ratio of 2D TMDC materials permits the physical adsorption (i.e., physisorption) of interacting molecules on the TMDC surface via non-covalent interactions and electron transfer processes that modify their resistance, rendering them suitable for electrochemical or gas sensing. 50 This multifunctionality and versatility in external stimuli that can be employed to modify the devices' resistance is useful in in-sensor computing architectures that offer higher integration density and lower fabrication complexity. These attributes are desirable in flexible light-weight multimodal sensing systems for wearable neuromorphic systems that could replace injured nerves or study sensory and central nervous system disorders, and for portable sensing devices for the Internet of Things (IoT).

However, there are challenges to overcome in order to reach higher performance, in terms of lower power consumption (the biological analogue imposes reaching <aJ levels on electronics), greater device stability and higher degree of scalability that will enhance their commercialisation potential. The material quality can be improved *via* optimised synthesis routes and additional post-synthesis

treatments to control the defect formation, such as annealing, plasma etching, and chemical functionalisation. More research focus should be placed on different types of heterostructures, such as 2D perovskites/TMDC, which present intriguing photophysics and band engineering potential, due to the tuneability of the organic spacer of the 2D perovskites.⁵¹ Twistronics has emerged as a novel approach for 2D materials to tune their optical and electrical properties (e.g., dielectric constant, refractive index, extinction and absorption coefficient) by modifying the rotation angles in the superposition of the periodic structures of the TMDC on each other, providing further flexibility for using the same material in different applications.⁵²

Additional device engineering methods, such as surface treatments and contact engineering can reduce the interlayer impurities and enhance the charge transfer kinetics. Scaling up the heterostructures apart from the single layers and system integration of the synaptic device arrays for real-world use will help unlock their full potential for future neuromorphic and human vision systems that are expected to revolutionise future computing, robotics, and wearable electronics.

Acknowledgements

Both authors wish to acknowledge the support from the UKRI Future Leaders Fellowship Grant (MR/V024442/1). D.G.G. also acknowledges support from European Union's HORIZON Europe Project TEAM-NANO under grant agreement No. 101136388.

Author Contributions

R.S.B. wrote the first draft and was responsible for the initial literature research. D.G.G. conceived and coordinated the work, reviewed, revised, edited the full text and compiled the final version after revisions.

Declaration of Interests

The authors declare no competing interests.

References

- 1. Jana, R., Ghosh, S., Bhunia, R., and Chowdhury, A. (2024). Recent developments in the state-of-the-art optoelectronic synaptic devices based on 2D materials: a review. Journal of Materials Chemistry C *12*, 5299-5338. https://doi.org/10.1039/D4TC00371C.
- 2. Jana, R., Ghosh, S., Bhunia, R., and Chowdhury, A. (2024). Recent developments in the state-of-the-art optoelectronic synaptic devices premised on 2D materials: A review. Journal of Materials Chemistry C *12*, 5299-5338. https://doi.org/10.1039/D4TC00371C
- 3. Lee, Y., Oh, J.Y., Xu, W., Kim, O., Kim, T.R., Kang, J., Kim, Y., Son, D., Tok, J.B.-H., Park, M.J., et al. (2018). Stretchable organic optoelectronic sensorimotor synapse. Science Advances 4, eaat7387. https://doi.org/10.1126/sciadv.aat7387.
- 4. He, H.-K., Yang, R., Zhou, W., Huang, H.-M., Xiong, J., Gan, L., Zhai, T.-Y., and Guo, X. (2018). Photonic Potentiation and Electric Habituation in Ultrathin Memristive Synapses Based on Monolayer MoS2. Small *14*, 1800079. https://doi.org/10.1002/smll.201800079.
- 5. Wang, J., Ilyas, N., Ren, Y., Ji, Y., Li, S., Li, C., Liu, F., Gu, D., and Ang, K.W. (2024). Technology and integration roadmap for optoelectronic memristor. Adv. Mater. *36*, 2307393. https://doi.org/10.1002/adma.202307393.
- 6. Sun, Y., Wang, D., and Shuai, Z. (2016). Indirect-to-Direct Band Gap Crossover in Few-Layer Transition Metal Dichalcogenides: A Theoretical Prediction. The Journal of Physical Chemistry C 120, 21866-21870. https://doi.org/10.1021/acs.jpcc.6b08748.
- 7. Tian, M.-Y., Gao, Y.-M., Zhang, Y.-J., Ren, M.-X., Lv, X.-H., Hou, K.-X., Jin, C.-D., Zhang, H., Lian, R.-Q., Gong, P.-L., et al. (2024). Toward direct band gaps in typical 2D transition-metal dichalcogenides junctions via real and energy spaces tuning. Communications Materials *5*, 188. https://doi.org/10.1038/s43246-024-00631-z.
- 8. Bernardi, M., Palummo, M., and Grossman, J.C. (2013). Extraordinary Sunlight Absorption and One Nanometer Thick Photovoltaics Using Two-Dimensional Monolayer Materials. Nano Lett. *13*, 3664-3670. https://doi.org/10.1021/nl401544y.
- 9. Tang, C.S., and Yin, X. (2024). Two-dimensional Transition Metal Dichalcogenides: A General Overview. In Two-Dimensional Transition-Metal Dichalcogenides, A. Wee, X. Yin, and C.S. Tang, eds. pp. 1-59. https://doi.org/10.1002/9783527838752.ch1.
- 10. Sun, Y., Wang, S., Zhang, Q., and Zhou, P. (2024). Evaluation of different 2D memory technologies for in-memory computing. Device 2, 100509. https://doi.org/10.1016/j.device.2024.100509.
- 11. Li, C., Sang, D., Ge, S., Zou, L., and Wang, Q. (2024). Recent Excellent Optoelectronic Applications Based on Two-Dimensional WS2 Nanomaterials: A Review. Molecules 29, 3341. https://doi.org/10.3390/molecules29143341.
- 12. Lin, L., Xu, Y., Zhang, S., Ross, I.M., Ong, A.C., and Allwood, D.A. (2013). Fabrication of luminescent monolayered tungsten dichalcogenides quantum dots with giant spin-valley coupling. ACS nano *7*, 8214-8223. https://doi.org/10.1021/nn403682r.
- 13. Ernandes, C., Khalil, L., Henck, H., Zhao, M.-Q., Chaste, J., Oehler, F., Johnson, A.T.C., Asensio, M.C., Pierucci, D., and Pala, M. (2021). Strain and spin-orbit coupling engineering in twisted WS2/graphene heterobilayer. Nanomaterials *11*, 2921. https://doi.org/10.3390/nano11112921.
- Zou, L.-R., Sang, D.-D., Yao, Y., Wang, X.-T., Zheng, Y.-Y., Wang, N.-Z., Wang, C., and Wang, Q.-L. (2023). Research progress of optoelectronic devices based on two-dimensional MoS2 materials. Rare Metals 42, 17-38. https://doi.org/10.1007/s12598-022-02113-y.
- 15. Wang, H., Li, C., Fang, P., Zhang, Z., and Zhang, J.Z. (2018). Synthesis, properties, and optoelectronic applications of two-dimensional MoS 2 and MoS 2-based heterostructures. Chem. Soc. Rev. 47, 6101-6127. https://doi.org/10.1039/C8CS00314A

- 16. Mahatha, S.K., Patel, K.D., and Menon, K.S.R. (2012). Electronic structure investigation of MoS2 and MoSe2 using angle-resolved photoemission spectroscopy and ab initio band structure studies. J. Phys.: Condens. Matter *24*, 475504. https://doi.org/10.1088/0953-8984/24/47/475504.
- 17. Yamamoto, M., Wang, S.T., Ni, M., Lin, Y.-F., Li, S.-L., Aikawa, S., Jian, W.-B., Ueno, K., Wakabayashi, K., and Tsukagoshi, K. (2014). Strong Enhancement of Raman Scattering from a Bulk-Inactive Vibrational Mode in Few-Layer MoTe2. ACS Nano *8*, 3895-3903. https://doi.org/10.1021/nn5007607.
- 18. Tongay, S., Sahin, H., Ko, C., Luce, A., Fan, W., Liu, K., Zhou, J., Huang, Y.-S., Ho, C.-H., Yan, J., et al. (2014). Monolayer behaviour in bulk ReS2 due to electronic and vibrational decoupling. Nature Communications *5*, 3252. https://doi.org/10.1038/ncomms4252.
- 19. Jariwala, B., Voiry, D., Jindal, A., Chalke, B.A., Bapat, R., Thamizhavel, A., Chhowalla, M., Deshmukh, M., and Bhattacharya, A. (2016). Synthesis and Characterization of ReS2 and ReSe2 Layered Chalcogenide Single Crystals. Chem. Mater. 28, 3352-3359. https://doi.org/10.1021/acs.chemmater.6b00364.
- 20. Rahman, M., Davey, K., and Qiao, S.-Z. (2017). Advent of 2D Rhenium Disulfide (ReS2): Fundamentals to Applications. Adv. Funct. Mater. 27, 1606129. https://doi.org/10.1002/adfm.201606129.
- 21. Xu, M., Xu, T., Yu, A., Wang, H., Wang, H., Zubair, M., Luo, M., Shan, C., Guo, X., and Wang, F. (2021). Optoelectronic synapses based on photo-induced doping in MoS2/h-BN field-effect transistors. Advanced Optical Materials *9*, 2100937. https://doi.org/10.1002/adom.202100937.
- 22. Islam, M.M., Dev, D., Krishnaprasad, A., Tetard, L., and Roy, T. (2020). Optoelectronic synapse using monolayer MoS2 field effect transistors. Scientific Reports *10*, 21870. https://doi.org/10.1038/s41598-020-78767-4.
- 23. Huang, P., Lukin, R., Faleev, M., Kazeev, N., Al-Maeeni, A.R., Andreeva, D.V., Ustyuzhanin, A., Tormasov, A., Castro Neto, A.H., and Novoselov, K.S. (2023). Unveiling the complex structure-property correlation of defects in 2D materials based on high throughput datasets. npj 2D Materials and Applications 7, 6. https://doi.org/10.1038/s41699-023-00369-1.
- 24. Jiang, J., Xu, T., Lu, J., Sun, L., and Ni, Z. (2019). Defect Engineering in 2D Materials: Precise Manipulation and Improved Functionalities. Research *2019*, 4641739. https://doi.org/10.34133/2019/4641739.
- 25. Chua, L. (1971). Memristor-the missing circuit element. IEEE Transactions on circuit theory *18*, 507-519. https://doi.org/10.1109/TCT.1971.1083337.
- Strukov, D.B., Snider, G.S., Stewart, D.R., and Williams, R.S. (2008). The missing memristor found. Nature 453, 80. https://doi.org/10.1038/nature06932.
- 27. Woo, K.S., Park, H., Ghenzi, N., Talin, A.A., Jeong, T., Choi, J.-H., Oh, S., Jang, Y.H., Han, J., Williams, R.S., et al. (2024). Memristors with Tunable Volatility for Reconfigurable Neuromorphic Computing. ACS Nano *18*, 17007-17017. https://doi.org/10.1021/acsnano.4c03238.
- 28. Zidan, M.A., Strachan, J.P., and Lu, W.D. (2018). The future of electronics based on memristive systems. Nature Electronics 1, 22-29. https://doi.org/10.1038/s41928-017-0006-8.
- 29. Gong, Y., Xing, X., Wang, X., Duan, R., Han, S.T., and Tay, B.K. (2024). Integrated Bionic Human Retina Process and In-Sensor RC System Based on 2D Retinomorphic Memristor Array. Adv. Funct. Mater. *34*, 2406547. https://doi.org/10.1002/adfm.202406547.
- 30. Sharmila, B., and Dwivedi, P. (2024). Wafer scale WS2 based ultrafast photosensing and memory computing devices for neuromorphic computing. Nanotechnology *35*, 425201. https://doi.org/10.1088/1361-6528/ad6006.
- 31. Ferrarese Lupi, F., Milano, G., Angelini, A., Rosero-Realpe, M., Torre, B., Kozma, E., Martella, C., and Grazianetti, C. (2024). Synaptic Plasticity and Visual Memory in a Neuromorphic 2D Memitter

- Based on WS2 Monolayers. Adv. Funct. Mater. *34*, 2403158. https://doi.org/10.1002/adfm.202403158.
- 32. Wang, H., Yang, J., Wang, Z., Shao, Y., Tang, Y., Guo, J., and Yan, X. (2024). Reconfigurable multifunctional neuromorphic memristor fabricated from two-dimensional ReSe2 ferroelectric nanosheet films. Applied Physics Reviews *11*, 011402. https://doi.org/10.1063/5.0170147.
- 33. Chen, Y., Huang, Y., Zeng, J., Kang, Y., Tan, Y., Xie, X., Wei, B., Li, C., Fang, L., and Jiang, T. (2023). Energy-efficient ReS2-based optoelectronic synapse for 3D object reconstruction and recognition. ACS Applied Materials & Interfaces 15, 58631-58642. https://doi.org/10.1021/acsami.3c14958.
- 34. Li, J., Zhou, Y., Li, Y., Yan, C., Zhao, X.-G., Xin, W., Xie, X., Liu, W., Xu, H., and Liu, Y. (2024). Perceiving the Spectrum of Pain: Wavelength-Sensitive Visual Nociceptive Behaviors in Monolayer MoS2-Based Optical Synaptic Devices. ACS Photonics 11, 4578-4587. https://doi.org/10.1021/acsphotonics.4c00877.
- 35. Novoselov, K.S., Mishchenko, A., Carvalho, A., and Castro Neto, A.H. (2016). 2D materials and van der Waals heterostructures. Science *353*, aac9439. https://doi.org/10.1126/science.aac9439.
- 36. Liao, W., Huang, Y., Wang, H., and Zhang, H. (2019). Van der Waals heterostructures for optoelectronics: Progress and prospects. Applied Materials Today *16*, 435-455. https://doi.org/10.1016/j.apmt.2019.07.004.
- 37. Ryu, Y.K., Frisenda, R., and Castellanos-Gomez, A. (2019). Superlattices based on van der Waals 2D materials. Chem. Commun. *55*, 11498-11510. https://doi.org/10.1039/C9CC04919C
- 38. Lin, Y., Wang, W., Li, R., Kim, J., Zhang, C., Kan, H., and Li, Y. (2024). Multifunctional optoelectronic memristor based on CeO2/MoS2 heterojunction for advanced artificial synapses and bionic visual system with nociceptive sensing. Nano Energy *121*, 109267. https://doi.org/10.1016/j.nanoen.2024.109267.
- 39. Li, Z., Zou, G., Xiao, Y., Feng, B., Huo, J., Peng, J., Sun, T., and Liu, L. (2024). MoS2/ZnO-heterostructured optoelectronic synapse for multiwavelength optical information-based sensing, memory, and processing. Nano Energy 127, 109733. https://doi.org/10.1016/j.nanoen.2024.109733.
- 40. Li, Y., Sun, H., Yue, L., Yang, F., Dong, X., Chen, J., Zhang, X., Chen, J., Zhao, Y., and Chen, K. (2024). Multicolor Fully Light-Modulated Artificial Synapse Based on P-MoSe2/PxOy Heterostructured Memristor. The Journal of Physical Chemistry Letters *15*, 8752-8758. https://doi.org/10.1021/acs.jpclett.4c01980.
- 41. Huang, F., Ke, C., Li, J., Chen, L., Yin, J., Li, X., Wu, Z., Zhang, C., Xu, F., and Wu, Y. (2023). Controllable resistive switching in ReS2/WS2 heterostructure for nonvolatile memory and synaptic simulation. Advanced Science *10*, 2302813. https://doi.org/10.1002/advs.202302813.
- 42. Xiao, Y., Li, W., Lin, X., Ji, Y., Chen, Z., Jiang, Y., Liu, Q., Tang, X., and Liang, Q. (2023). 2D MoTe2/MoS2–xOx Van der Waals heterostructure for bimodal neuromorphic optoelectronic computing. Advanced Electronic Materials *9*, 2300388. https://doi.org/10.1002/aelm.202300388.
- 43. Qiu, D., Zheng, S., and Hou, P. (2024). Simulating and Implementing Broadband van der Waals Artificial Visual Synapses Based on Photoconductivity and Pyroconductivity Mechanisms. ACS Applied Materials & Interfaces 16, 53142-53152. https://doi.org/10.1021/acsami.4c10128.
- 44. Jiang, D., Liu, Z., Xiao, Z., Qian, Z., Sun, Y., Zeng, Z., and Wang, R. (2022). Flexible electronics based on 2D transition metal dichalcogenides. Journal of Materials Chemistry A *10*, 89-121. https://doi.org/10.1039/D1TA06741A.
- 45. Chung, Y.Y., Chou, B.J., Hsu, C.F., Yun, W.S., Li, M.Y., Su, S.K., Liao, Y.T., Lee, M.C., Huang, G.W., Liew, S.L., et al. (2022). First Demonstration of GAA Monolayer-MoS2 Nanosheet nFET with 410μA μ m ID 1V VD at 40nm gate length. 2022 International Electron Devices Meeting (IEDM), 34.35.31-34.35.34. https://doi.org/10.1109/IEDM45625.2022.10019563.

- 46. Huyghebaert, C., Schram, T., Smets, Q., Agarwal, T.K., Verreck, D., Brems, S., Phommahaxay, A., Chiappe, D., Kazzi, S.E., Lockhart de la Rosa, C., et al. (2018). 2D materials: roadmap to CMOS integration. 2018 IEEE International Electron Devices Meeting (IEDM), 22.21.21-22.21.24. https://doi.org/10.1109/IEDM.2018.8614679.
- 47. Kim, S.J., Lee, H.-J., Lee, C.-H., and Jang, H.W. (2024). 2D materials-based 3D integration for neuromorphic hardware. npj 2D Materials and Applications 8, 70. https://doi.org/10.1038/s41699-024-00509-1.
- 48. Raza, A., Hassan, J.Z., Ikram, M., Ali, S., Farooq, U., Khan, Q., and Maqbool, M. (2021). Advances in Liquid-Phase and Intercalation Exfoliations of Transition Metal Dichalcogenides to Produce 2D Framework. Advanced Materials Interfaces 8, 2002205. https://doi.org/10.1002/admi.202002205.
- 49. Chen, C., Zhou, Y., Tong, L., Pang, Y., and Xu, J. (2025). Emerging 2D Ferroelectric Devices for In-Sensor and In-Memory Computing. Adv. Mater. *37*, 2400332. https://doi.org/10.1002/adma.202400332.
- 50. Hassan, J.Z., Raza, A., Din Babar, Z.U., Qumar, U., Kaner, N.T., and Cassinese, A. (2023). 2D material-based sensing devices: an update. Journal of Materials Chemistry A *11*, 6016-6063. https://doi.org/10.1039/D2TA07653E.
- 51. Baranowski, M., Surrente, A., and Plochocka, P. (2022). Two Dimensional Perovskites/Transition Metal Dichalcogenides Heterostructures: Puzzles and Challenges. Isr. J. Chem. *62*, e202100120. https://doi.org/10.1002/ijch.202100120.
- 52. Gupta, N., Sachin, S., Kumari, P., Rani, S., and Ray, S.J. (2024). Twistronics in two-dimensional transition metal dichalcogenide (TMD)-based van der Waals interface. RSC Advances *14*, 2878-2888. https://doi.org/10.1039/D3RA06559F.
- 53. Xue, G., Qin, B., Ma, C., Yin, P., Liu, C., and Liu, K. (2024). Large-Area Epitaxial Growth of Transition Metal Dichalcogenides. Chem. Rev. 124, 9785-9865. https://doi.org/10.1021/acs.chemrev.3c00851.
- 54. Jadhav, J., Waghadkar, Y., Padwal, Y., Hashem, M., Fouad, H., Kekade, S.S., Terashima, C., Chauhan, R., Charhate, S., Gosavi, S.W., and Late, D.J. (2024). Enhanced dye degradation using 2H-MoS2 and 1T@2H-MoS2: A comparative study. J. Solid State Electrochem. https://doi.org/10.1007/s10008-024-05813-w.
- 55. Sathyanarayana, S., and Das, B.C. (2024). Grain boundary effect unveiled in monolayer MoS 2 for photonic neuromorphic applications. Journal of Materials Chemistry C *12*, 13827-13839. https://doi.org/10.1039/D4TC02912G

Figure Titles and Legends

Figure 1. Transition metal dichalcogenide materials and their monolayer structures

- (A) Periodic table of the known experimentally synthesised layered transition metal dichalcogenide materials with a summary of their existing structural phases (H: trigonal prismatic, T: octahedral, T': distorted octahedral, T_d: orthorhombic), typical band gaps (values at the bottom left corner of each grid, M: metallic), and observed electronic phases (superconducting, topological, and charge density wave CDW). Adapted from⁵³.
- (B) 2H trigonal prismatic and 1T octahedral coordination of metal atoms in the unit cell of MoS₂ monolayer structure.⁵⁴

Figure 2. Synaptic functionalities of a retinomorphic WS₂ memristive device²⁹

- (A) Schematic illustration of human vision system.
- (B) Schematic of WS₂ retinomorphic memristive device.
- (C) EPSC response induced by RGB light stimuli.
- (D) Short- and long-term plasticity (potentiation) behaviour of WS₂ memristive device upon illumination with 637 nm wavelength pulses.
- (E) Variation in paired-pulse facilitation (PPF) with different pulse intervals.
- (F) Long-term potentiation characteristics observed for different wavelengths of light.

Figure 3. Wavelength-sensitive visual response characteristics of a nociceptor type of device³⁴

- (A) The device exhibits photocurrent responses at 320 nm under varying light intensities, showing a clear threshold behaviour.
- (B) The device's threshold response varies depending on the wavelength of the incident light, showcasing its wavelength sensitivity.
- (C) No-adaptation behaviour of device at different intensity levels, and (D) different wavelengths.
- (E) The device demonstrates relaxation responses with varying time intervals between the pulses and (F) with varying wavelength.

(G) Illustration of allodynia (pain from non-painful stimuli) and hyperalgesia (increased sensitivity to pain) with varying stimulus intensity and (H–K) wavelength-sensitive pain responses. The device mimics hyperalgesia and allodynia at different wavelengths.

Figure 4. Operating mechanism of a van der Waals heterostructure optoelectronic memristor Adapted from⁴².

- (A) Illustration of the structure of a $MoTe_2/MoS_{2-x}O_x$ memristor operating in optical and electronic mode and zoomed-in region of the molecular structure of a vertical heterostructure stack.
- (B) Resistive switching mechanism of MoTe₂/MoS_{2-x}O_x memristors:
- i) Distribution of the atoms of the elements within the heterostructured device in the initial state and the migration trends of oxygen and sulphur ions under positive bias towards the positive electrode.
- ii) Ion aggregation in the heterojunction stacking region under forward bias and the appearance of oxygen vacancies and sulphur vacancies in the MoTe₂/MoS_{2-x}O_x interface region forming a conducting filament (LRS, SET).
- iii) Ion migration towards the opposite direction and vacancy filling under negative bias (HRS, RESET).

Table 1. Performance comparison of 2D TMDC-based optoelectronic synaptic devices

Material	Synthesis of TMDC	Wavelength [nm]	PPF [%]	Power consumption nJ	Accuracy rate (%)	Ref
A. Single TM	IDC layer devices					
	Exfoliation	435	~170	5		29
WS_2		520	-	12	100	
		637	-	18		
WS_2	Sulphurisation	950	-	-	98.27	30
1L WS2	CVD	520	102	-	-	31
		320	57.8	-	-	34
17.37.0	Mechanical	405				
1L MoS ₂	exfoliation	532				
		638				
MoS_2	CVD	532	~116	-	-	55
ReS_2	Mechanical exfoliation	450-805	124	1.212 ×10 ⁻⁵	97.0	33
ReSe ₂	Solid-phase	405				
	sintering and	520	-	-	97.4	32
	spin-coating	650				

B. Heterostructures

		UV				
CeO ₂ /MoS ₂	Hydrothermal	520	25	-		38
		580				
		620			-	
P-MoSe ₂ /P _x O _y	Selenisation	470	3.35			
		590				40
		655	2.58			10
		808		-		
		375	149			
MoS ₂ /ZnO		490	159			
	Mechanical	525	164	2.55	-	39
	exfoliation	625				
		800				
$MoTe_2/MoS_{2-x}O_x$	Mechanical	532-1064	-	-	05.2	42
	exfoliation				95.3	
MoS ₂ /WSe ₂	Mechanical exfoliation	660	-	3 ×10 ⁻⁴		
		1064	66.7	1. 1×10 ⁻³		43
		1550	41.8	4×10 ⁻⁴	-	
ReS ₂ /WS ₂	CVD	532				
		690	-	-	-	41
		070				

Figures

Figure 1

A





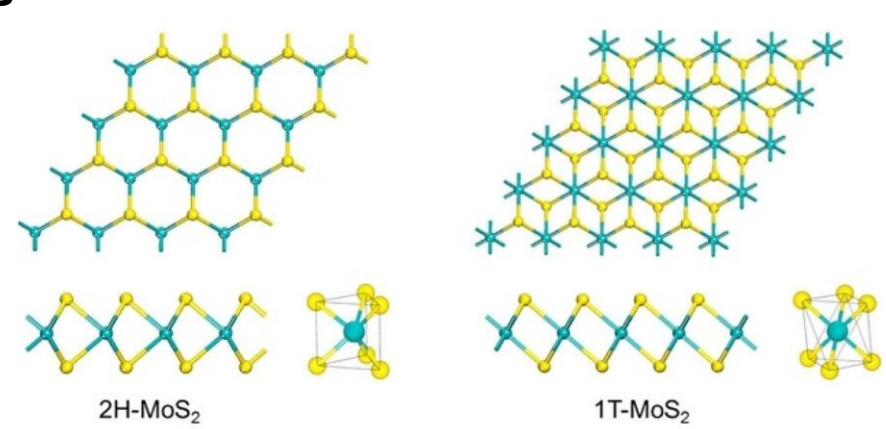


Figure 2

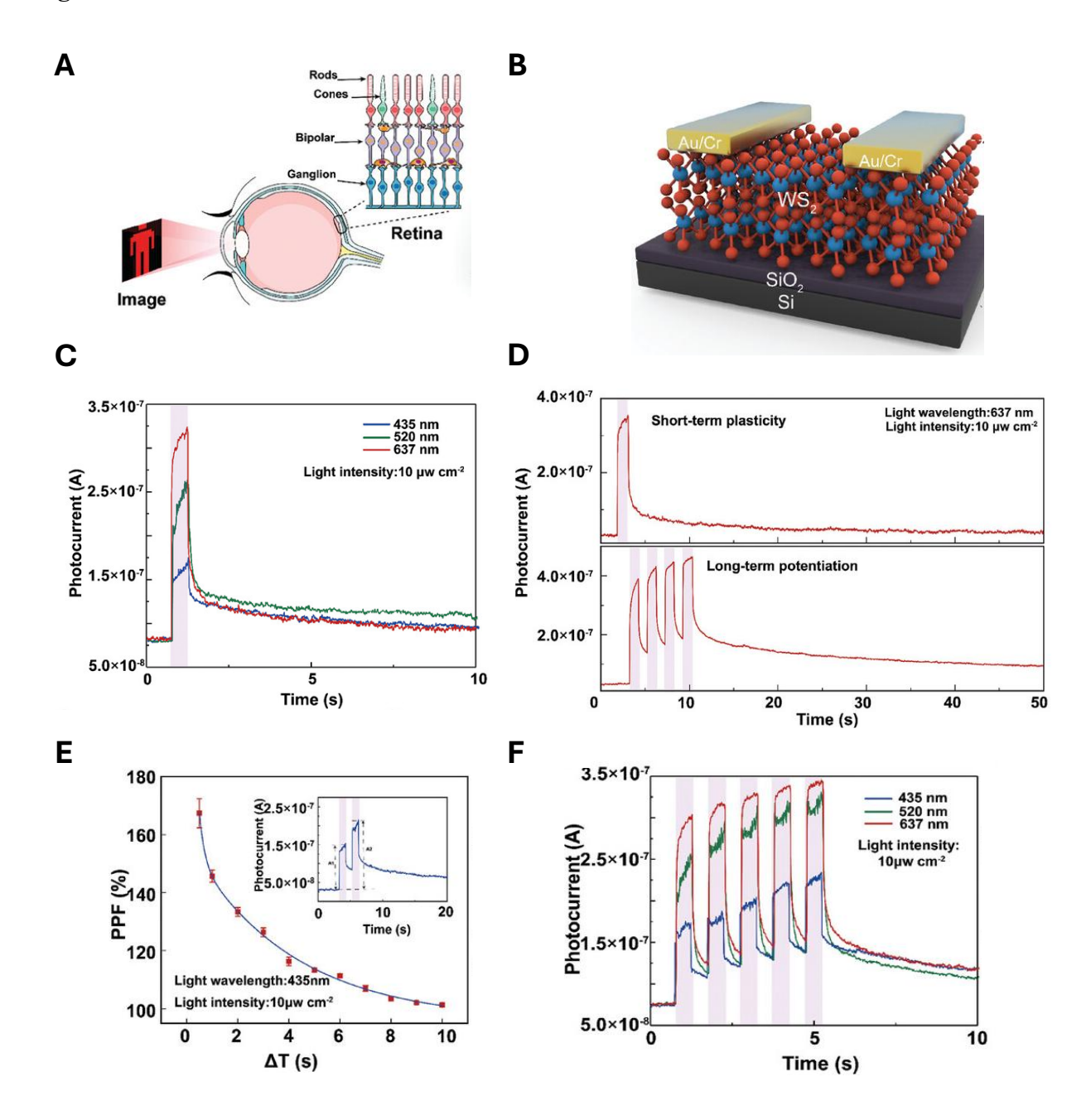


Figure 3

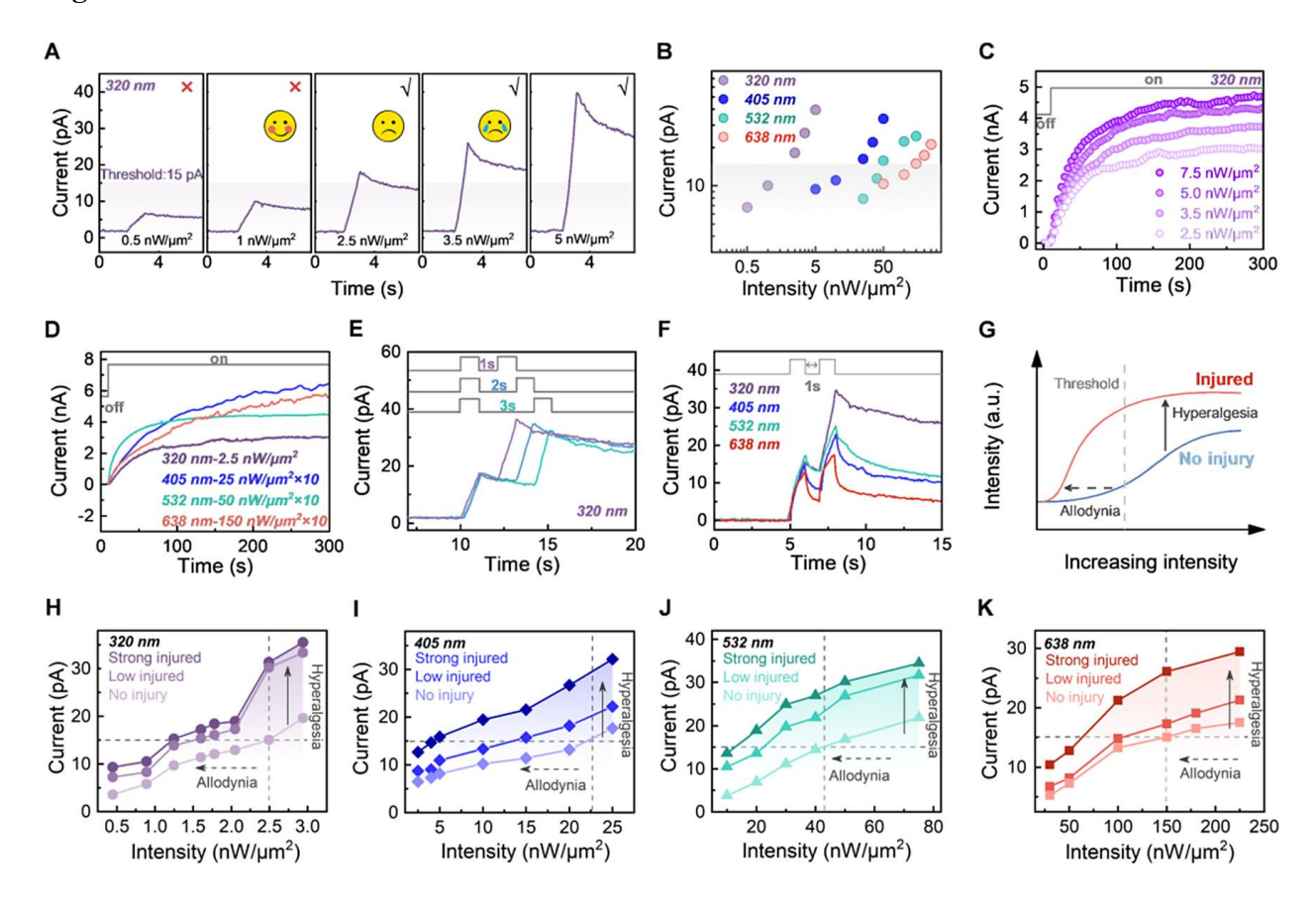


Figure 4

